Design of an Adiabatic Calorimeter for Cementitious Mixtures by Multi-Objective Optimization

Jhonatan A. Becerra-Duitama[1,*], Mauricio Mauledoux[2], Óscar F. Avilés[2]

[1]Faculty of Engineering and Basic Sciences, Juan de Castellanos University, Tunja, Colombia

[2]Faculty of Engineering, Military University Nueva Granada, Bogotá, Colombia

Abstract

This study aims to design an adiabatic calorimeter for cementitious mixtures using NSGA-II and the Pareto optimal solution set. In this multi-objective optimization, the controller effort and heating time are selected as objective functions. Likewise, the volume and the material to be heated were chosen as decision variables. The optimal solution was selected using Nash bargaining methods. After implementing the optimal solution, the Wilcoxon test was applied to statistically validate the developed work. The measurements performed were compared with other research and it was observed an improvement in the measurement of heat of hydration in cementitious mixtures. Also, it was noted a decrease in the error in the temperature measurement.

1. Introduction

Nowadays, the measurements of the heat of hydration in cementitious mixtures are required. For this purpose, some equipment has been developed over the years to perform these tests. The most commonly used devices to determine the heat of hydration in cement mixtures are isothermal, semi-adiabatic, and adiabatic calorimeters. The latter is the least used because it is complicated and costly to manufacture, and its correct operation requires high sensitivity [1]. Nevertheless, it is the most accurate method and provides the best measurements [2]. For this reason, methods based on concurrent engineering were applied, to develop a low-cost and easy-to-acquire calorimeter.

Concurrent design can be applied to develop any project in a cross-functional manner bearing in mind all stages of the product life cycle, from manufacturing to final disposal [3-5]. Additionally, the concurrent design reduces production costs and time to market while increasing product quality. Deshpande [6] mentions that various companies such as Hewlett-Packard, Texas Instruments, General Motors, and Motorola have successfully implemented concurrent engineering projects. Among the benefits obtained, can be noted: a 55 % reduction in time to market, a 70 % increase in performance, and a 350 % increase in quality. In addition, Kügler et al. [7] found a reduction in production time from 30 to 18 months in the development of a new minicomputer. Wang and Feng [8] indicated that implementing concurrent design procedures in companies reduced the number of design changes by 50 %, shortened product design time by 40 % to 70 %, and decreased waste generated by 75 %.

Previously this study, this type of concurrent design methodology had not been used to develop adiabatic calorimeters for cement mixtures, even considering the existing problems with these devices. The first problem is the control system that has a low response time, Prasath and Santhanam [9] described how the developed calorimeter took about one hour to reach the

---

* Corresponding author. E-mail address: jalexanderbecerra@jdc.edu.co

established reference. The second problem is a high working sensitivity and good insulating material are necessary for the heat transfer to be close to zero, allowing for higher accuracy in the measured data [10]. The third problem is the high production cost, making it a commercially nonviable and quite exclusive device [11].

For the above-mentioned reasons, methods based on concurrent design were implemented, to design a low-cost and easy-to-obtain calorimeter. Therefore, it was used a multi-objective optimization algorithm, which took into account all aspects of the system's operation. To achieve the optimal design, the non-dominated sorting genetic algorithm II (NSGA-II) was used to determine the parameters, dimensions, and materials required for the design of the adiabatic calorimeter [12]. Likewise, it was implemented the calorimeter designed to perform heat of hydration measurements on cement paste samples. The novelty of this work is to display that the calorimeter was developed using concurrent design (optimization algorithms) unlike existing calorimeters implemented [13-16]. It is expected that this work will be one of the first to develop optimized calorimeters for cement mixtures [17].

2. Methods

This section describes the development of the project, which was divided into three parts. The first part is the implementation of the optimization algorithm, for which the non-dominant sorting genetic algorithm (NSGA-II) was used. It is important to point out that, before implementing the NSGA-II algorithm, two evolutionary algorithms were tested. The evolutionary algorithms used were: The Multiobjective Differential Evolution (MODE) algorithm [18] and the Differential Evolution Multiobjective Optimization (DEMO) algorithm [19]. However, due to the nature of the calorimeter, the two algorithms could not be implemented, because the optimization problem had mixed variables, since one objective function had to choose the insulating material (something tangible), and the other objective function had to choose the physical dimensions of the calorimeter (numbers). Also, implementing either of the two evolutionary algorithms would have required transforming the objective functions so that both were under the same conditions. This would have introduced imprecision and inaccuracy in the results obtained. For this reason, the NSGA-II algorithm was chosen, since it did allow working with mixed variables.

The objective functions to take into account were the environment to be heated and the cumulative error of the measurement. By applying the algorithm and the two objective functions, the Pareto front was determined, by which the solution to be implemented was chosen. Hence, it was needed to apply bargaining methods. The methods used were the Nash method and the egalitarian method. The second part of the project involved the design and implementation of the control system from simulation to its commissioning. Finally, the culmination of the third part of the project was focused on the construction of the adiabatic calorimeter, bearing in mind the design parameters calculated in the previous parts. In addition, some tests were carried out with cement paste specimens, verifying the correct operation by checking with other similar studies. Fig. 1 shows the schematic diagram where the design steps are represented.
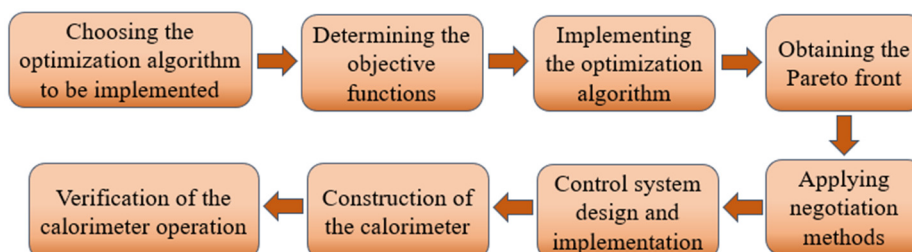

Fig. 1 Schematic diagram of the design process

2.1. Algorithm optimization

To obtain the best solution for the problem, it was adopted the non-dominant sorting genetic algorithm (NSGA-II) taken from Kalami [20]. The parameters of the algorithm employed are shown in Table 1. Before implementing the optimization

algorithm, it was established the objective functions that governed the selection of the optimal calorimeter design. It is worth noting that the first function chosen depends directly on the thermal process. The parameters and materials included in this function were selected based on the physical nature of the process. Moreover, this function was established to minimize the heating time of the environment to be controlled.

Table 1 NSGA-II parameters

P1	P2	P3	P4	P5
100	100	0.7	0.4	0.02

where P1 is the maximum number of iterations, P2 is the population size, P3 is the crossover percentage, P4 is the mutation percentage, and P5 is the mutation rate.

Additionally, the second objective function was defined as the minimization of the cumulative error in the measurement. As can be seen, the behavior of the two functions is conflicting, since to achieve a short warm-up time, the controller must act quickly. Therefore, finding the right balance between both functions was required to obtain the optimal design. The followings are the objective functions and the decision variables proposed for the development of the project.

Objective function 1 ($f1$) is intended to minimize water heating time. The heating time in terms of heat generated and power delivered to the system is expressed as

$$
\begin{aligned}
f1 &= t \\
&= Q/P \\
&= \rho \times V \times Cespecific \times \Delta T / P
\end{aligned}
\tag{1}
$$

where t is time (s), Q is generated heat (J), P is heating element power (W), ρ is the density of the chosen substance (kg/m3), V is the volume of the vessel containing the substance (m3), $Cspecific$ is the specific heat of the substance (J/kg°C), and ΔT is temperature variation (°C).

Decision variables: the calorimeter material and dimensions were setting it up as decision variables. Table 2 shows the materials proposed as insulation for the calorimeter and their characteristic values.

Table 2 Proposed materials for calorimeter insulation

Material	Specific heat Ce (J/kg°C)	Density (kg/m3)
M1	4186	1000
M2	3730	1035
M3	3300	1053
M4	1	1.239

where M1 is Water, M2 is water and coolant at 50%, M3 is water and coolant at 30%, and M4 is air. As the refrigerant Ethylene glycol was chosen. The proposed dimensions are set out in Table 3:

Table 3 Proposed calorimeter dimensions

Volume (L)	Width (cm)	Length (cm)	Height (cm)
15	24	22	28
25	30	26	32
30	30	31	32
35	30	32	36

Objective function 2 ($f2$) is intended to minimize cumulative measurement error. To ensure minimal error, it was called to simulate the response of the controller, to establish the best parameters to be implemented. The simulation was performed using MATLAB software. First, the mathematical model of the thermal system to be controlled was set up. The differential equation representing the thermal system is expressed as:

$$\frac{dT}{dt} = \frac{P \times T}{\rho \times V \times Cp} \tag{2}$$

Afterward, the type of controller to be implemented could be designed and simulated. The input variable is voltage and the output variable is temperature. The controller was determined using the sliding mode method. The sliding surface proposed for the controller utilized is represented by

$$\sigma = x_1 + k_0 \int x_1 - x_d \tag{3}$$

The equivalent controller and the attractive controller are respectively defined as

$$Ueq = \frac{\rho \times V \times Cp}{I \times t} \times -k_0 \left(x_1 - x_d \right) \tag{4}$$

$$U_N = \frac{\rho \times V \times Cp}{I \times t} \times L \times \mathrm{sgn}(\sigma) \tag{5}$$

After that, it was determined the cumulative error of the controller using Simulink and MATLAB. For this purpose, it was established the value of the constant k0 present in Eqs. (3)-(4), based on the previously defined decision variables. Fig. 2 shows the method to identify the cumulative error of the controller. It can be seen that the study signal is the input signal, which is the temperature in the cement sample. Likewise, it can be seen in the sliding mode representation of the controller. The orange color represents the attractive control, while the fuchsia color represents the equivalent control. Sliding mode control provides a systematic approach to the problem of maintaining accuracy, stability, adjustability, and performance in the face of model inaccuracy. It is also an efficient tool for designing robust controllers for complex nonlinear and multivariable plants. There are two main advantages of this type of control. First, the dynamic behavior of the system can be adapted by the particular choice of a slip function. Secondly, the closed-loop response becomes insensitive to some particular uncertainties.
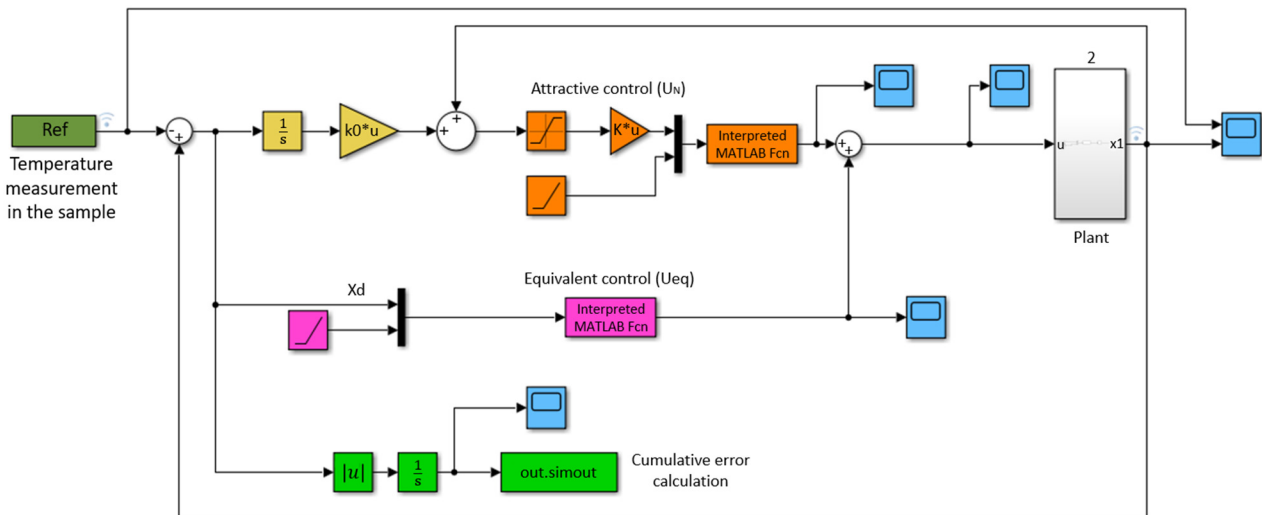

Fig. 2 Computation of the cumulative error of the controller

When the algorithm finishes its process, it displays the set of optimal solutions, entitled the Pareto front. Because all the values obtained are possible answers, it is necessary to apply bargaining methods to obtain the choice criterion. The negotiation methods used to find the selected solution to manufacture the calorimeter were the egalitarian method and the Nash method [21].

2.2. Construction of the calorimeter

After applying the optimization algorithm, the control system was designed and implemented. As mentioned previously, the controller design was selected using sliding modes. To fully understand the behavior of the control system, it is important

to mention the various parts and the operation of the calorimeter. The part where the measurement was carried out is a cubic acrylic container with a side length of 35 cm (Fig. 3(a)). The cement sample was contained inside a 10 cm box (Fig. 3(b)). This box has an extended lid that allows the sensor to enter the sample. In turn, the sample is housed inside the small box and contained inside the large container (Fig. 3(c)).
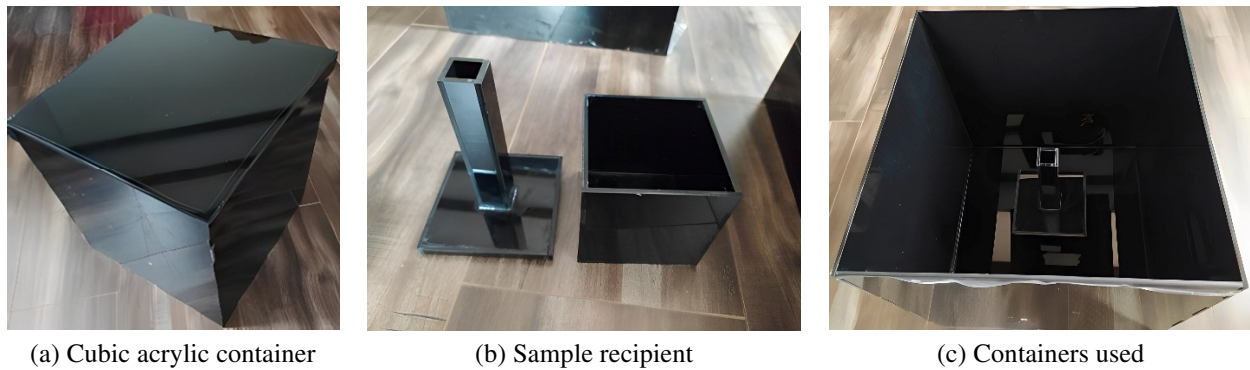

| (a) Cubic acrylic container | (b) Sample recipient | (c) Containers used |

Fig. 3 Vessels used for calorimeter measurement

Moreover, to ensure minimal heat loss, the water temperature was controlled by three separate systems. The first is a temperature homogenization system, which mixed the water so that the temperature was approximately the same throughout the volume. This system has two mixing paddles operated by electric motors. The functioning of this system is independent of the variation of the temperature in the calorimeter, so that, as soon as it is started, the paddles are activated. The second is the heating system, which consists of two heating resistors (Fig. 4). The actuators of these two systems are located on the cover of the main box. In turn, the calorimeter has 3 temperature sensors, 1 for the sample and 2 for water temperature measurement.
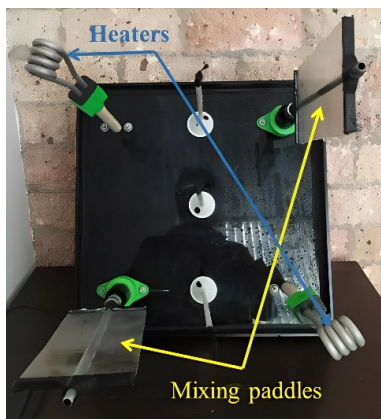

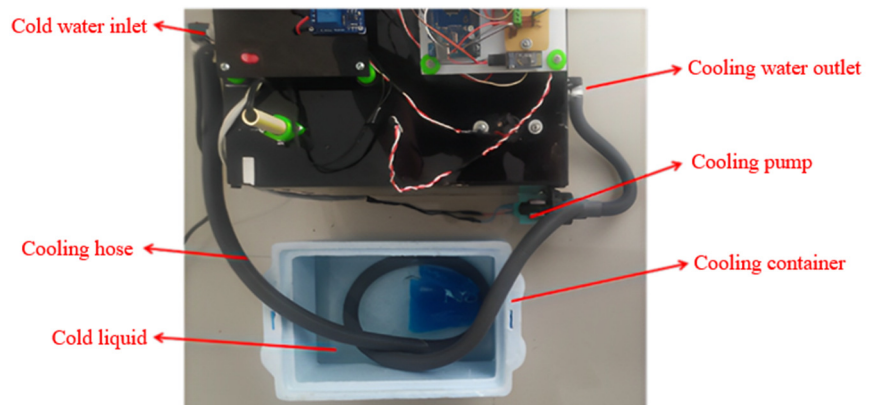Fig. 4 Mixing paddles and heaters

Fig. 5 Cooling system

The third and last system was the cooling system. This has a pump that allows the flow of water to an external container filled with cooling liquid, to reduce the calorimeter's ambient temperature through heat exchange, Fig. 5. It can be observed that the heating and cooling systems depend on the temperature of the sample (reference temperature). When the sample temperature is below the ambient temperature, the cooling system is activated; consequently, when the sample temperature is above the ambient temperature, the heating system must be activated. To measure temperature changes, submersible NTC 10k sensors were used.

In addition to the three systems mentioned above, the calorimeter has power and a control element. Fig. 6 shows these components. The power element consists of relays (a) that allow the activation or deactivation of the heating and cooling system actuators. Also, the control element includes a microcontroller (Arduino MEGA) (b), an electronic conditioner for the sensors (c), a Bluetooth module for data acquisition (d), and a module for data storage using micro-SD memory (e). Fig. 7 shows the calorimeter modeled in Solidworks, where the different components and systems that are part of the developed device can be seen more clearly.
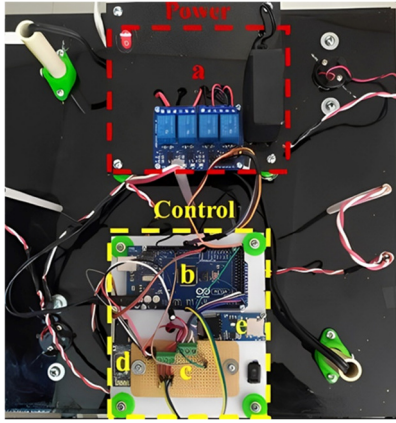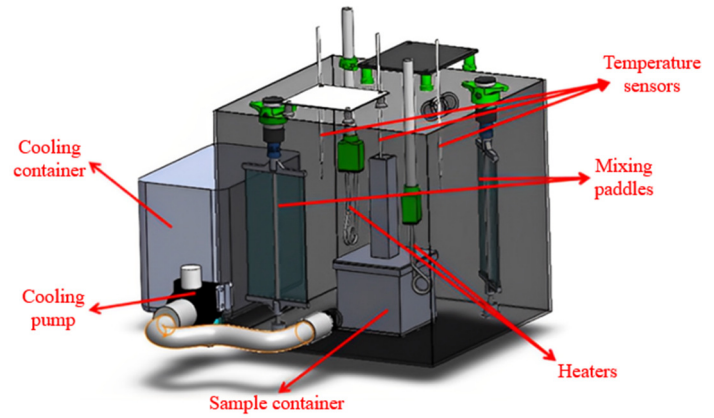
Fig. 6 Power and control part

Fig. 7 Calorimeter developed

3. Results and Discussion

As a result of using the optimization algorithm (NSGA-II), it was obtained a set of solutions or Pareto front. To achieve this, the algorithm was implemented with a population of 100 individuals, Fig. 8. The behavior of the Pareto front is consistent with the definition of the two objective functions since the system is a minimization problem and its shape must be convex. This generates a conflict in the possible solution; because, for the heating time to be minimal, the cumulative error of the controller must be large, and, by contrast, for the cumulative error of the controller to be reduced, the heating time must be increased. Convex Pareto fronts are obtained with a set of acceptable multi-objective optimization solutions and satisfying the objective functions [22-24].
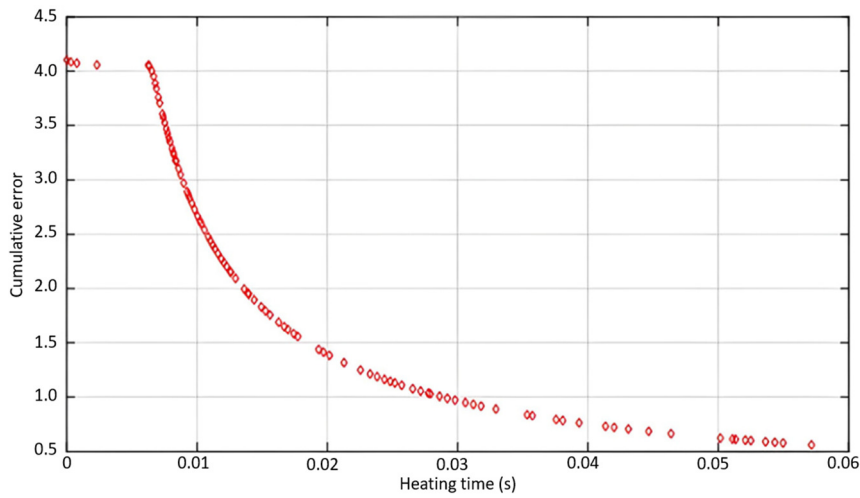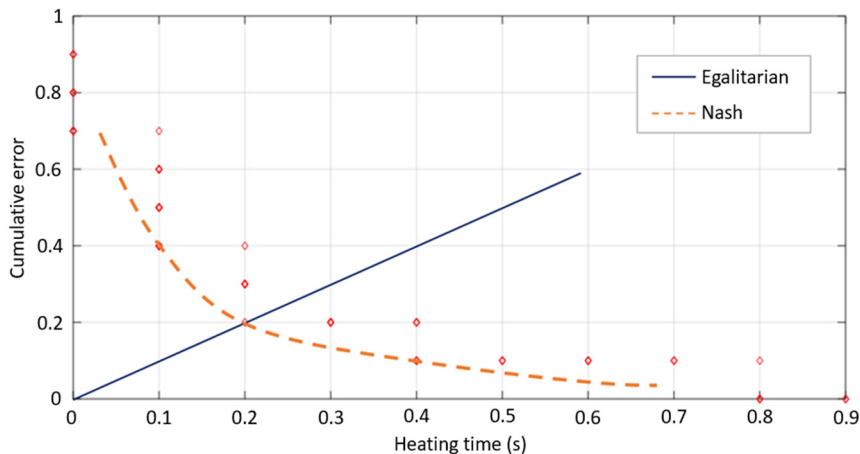

Fig. 8 Pareto front

Fig. 9 Nash and egalitarian negotiation methods

For a better analysis of the results obtained, it was needed to normalize the Pareto front, reduce the number of decimal places and obtain simpler values to analyze. It should be noted that the points appear in this way in the graph because the data were filtered and only normalized data (values between 0 and 1) appear. It is important to note that the data processed by the NSGA-II algorithm has the solutions to the proposed problem or the decision variables, that is, the genotype. As a result of collecting this data, the response of the objective functions of the problem, represented by the Pareto front, meaning the phenotype, was found. To obtain the best design (the best solution), it was required to establish the genotype, so bargaining methods were used, which are aimed to find a better decision. Fig. 9 shows the Pareto front with the two negotiation methods used.

By applying the bargaining methods, it can be evidenced they pass over 3 coordinate points. The egalitarian bargaining method goes through the coordinate point (0.2, 0.2), while the Nash bargaining method goes through the coordinate points (0.1, 0.4), (0.2, 0.2), and (0.4, 0.1). The optimal values of the phenotype and genotype are shown in Table 4. As previously mentioned, the decision variables selected were the volume and type of material to be heated. The optimal material to heat is water; with the volume varying between 18 and 30.5 liters. It is highlighted these values were the result of the data processing performed by the NSGA-II algorithm.

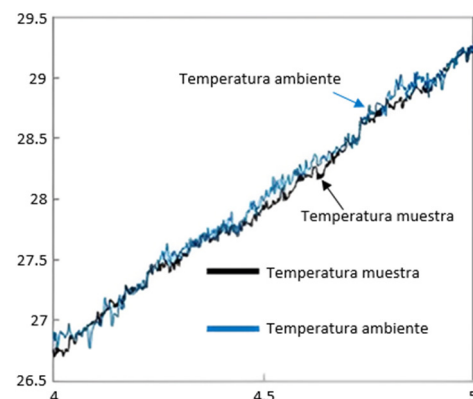Table 4 Decision variables obtained by the negotiation methods.

Phenotype	Negotiation methods	Decision variables (Genotype)	
		Volume (L)	Materiales to be heated
(0.1, 0.4)	Nash	18	Water
(0.2, 0.2)	Equal/Nash	30.5	Water
(0.4, 0.1)	Nash	27.4	Water

Despite the fact all three solutions were optimal, a water volume of 18 liters was finally chosen. This choice was made to minimize the costs in the manufacture of the calorimeter, since the smaller the dimensions, the lower the manufacturing cost. It is clarified the choice of the final design will depend on the designer's criteria and on some factors not considered in the algorithm, such as costs, physical space, portability, and sample size, among others. The calorimeter's dimensions were made slightly larger than the volume of water to be heated so that all the components could be positioned comfortably and practically.

As mentioned before, the control system was designed using sliding modes. This type of control is composed of two parts. The first part is the equivalent control; which has the function of restricting the reference temperature to the chosen non-stick surface. The second method is the attractive control, aimed at preventing the reference temperature from deviating from the desired trajectory, thus attracting it to the calculated non-stick surface.
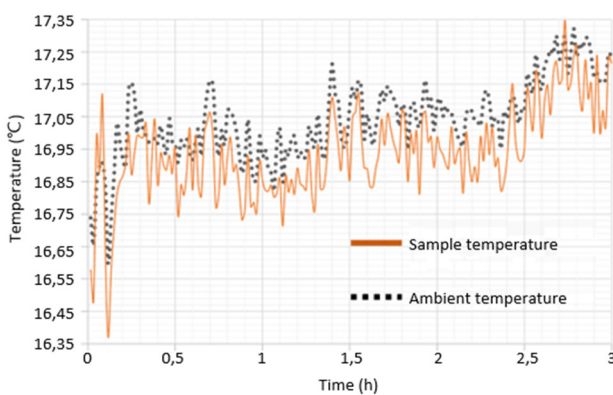
(a) Error obtained with concurrent design   (b) Error obtained within Lin [25]

Fig. 10 Error obtained in the tests

After verifying the design of the controller was correct, it was then implemented. Fig. 10(a) shows the reference temperature variation (orange curve) and the water temperature (black curve). It is observed that the difference between the reference temperature and the water temperature did not exceed 0.2 °C/h. Compared with Lin [25], the relationship in the

change of temperatures is similar, as shown in Fig. 10(b), and the temperature loss has less variation; this is a result of the concurrent design used. It is noted the system to be controlled is a thermal system and the response of these systems is slow due to the nature of the system itself.

To assure the calorimeter's proper functioning, three tests were carried out using identical cement paste mixtures. The main characteristics of the mixture employed were; 50 g of cement, 35 ml of water, a water/cement ratio of 0.7, and a total volume of 24.74 cm^3. Fig. 11 shows the temperatures obtained for each test. It is seen that the difference between the ambient temperature and the temperature of the sample was quite minimal (about 0.2 °C). However, the temperature of the sample increases as time goes by, because of the chemical nature of the cement. The temperature values obtained are related to the size of the sample; it is important to keep in mind that using a smaller mass will result in a smaller temperature variation.
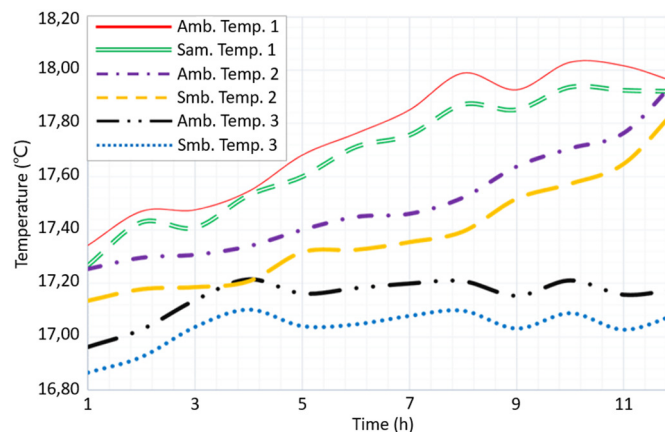

Fig. 11 Measured temperatures

To verify that the variation in ambient temperature versus sample temperature is statistically acceptable, the Wilcoxon test was used to verify the results obtained. For this purpose, it was defined the null hypothesis and the alternative hypothesis as:

Null hypothesis (H0): The curves obtained are not acceptable.

Alternative hypothesis (H1): The curves obtained are acceptable.

To obtain the values of the parameters p and h, the data used to obtain the curves in Fig. 11 and Matlab were used. Table 5 shows the data obtained by applying the Wilcoxon test:

Table 5 Values obtained from Wilcoxon test

Temperature	p	h
ΔT1 vs ΔT2	0.00024	1
ΔT1 vs ΔT3	0.0166	1
ΔT2 vs ΔT3	0.00006	1

The ΔT values correspond to the difference between the sample temperature and the ambient temperature for each measurement taken (T1, T2, and T3). In other words, the value considered was the error in the measurement, since the main objective of the calorimeter is that the difference between temperatures is as close to zero as possible. It can be seen that the p < 0.05 and the value of h = 1 for all the measurements made, therefore the null hypothesis is rejected and the alternative hypothesis is accepted.

Fig. 12 shows the heat of hydration curves obtained for each measurement. The behavior of the three curves was similar, with a slight difference between the maximum values. Furthermore, the maximum heat peak occurred approximately 2 hours after the test. The curves obtained are based on the temperatures measured in the calorimeter, the mathematical model that governs the behavior of these curves is part of another study, however, it was important in establishing the behavior of the

hydration heat. It is important to clarify that, even though the sample conditions were the same for each measurement, cement hydration is a chemical process that is not exact and is approximated by mathematical models; therefore, the results obtained in Fig. 12 are not the same, but its performance is in line with what is reported in the literature.

The resulting curves were compared to some similar investigations. In Chidiac and Shafikhani [26], the heat of the hydration curve was obtained for different types of cement mortar mixtures, which means the number of samples used was higher than in the present work. The maximum peak was achieved approximately 9 hours after the start of the measurement and heat of hydration values between 0.5 and 4.0 W/g were obtained. The measurement time was 26 hours.
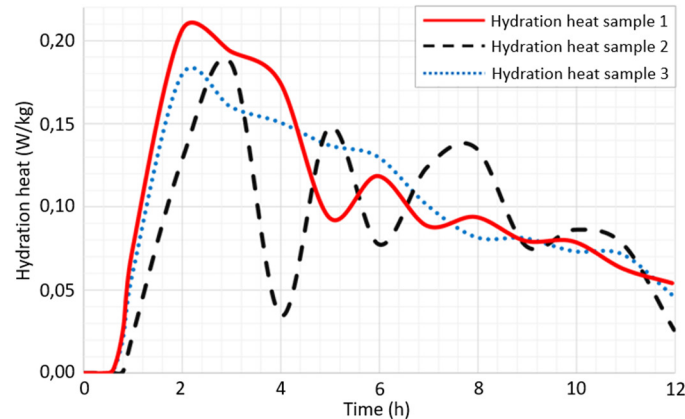

Fig. 12 Hydration heat curves obtained

Additionally, Sanderson et al. [1] evaluated the behavior of the hydration heat in cement mortars with a sample volume of 125 cm^3. The values of the heat of hydration oscillate between 0.0005 W/g and 0.004 W/g, and the maximum peak is reached almost 12 hours after testing. The measurement time was 24 hours. Besides, in Lin and Chen [27] cubic concrete specimens of 5.8 m^3 volume were made. The measurement time was 144 hours. The maximum heat peak was 3.7 W/kg and the time to reach it was approximately 9 hours. Additionally, in Prasath and Santhanam [9], the heat of the hydration curve was obtained for concrete samples with a volume of 5300 cm^3 approximately, and the measurement time was approximately 40 hours. The maximum heat peak was 4.8 W/kg and was reached 10 hours after the start of the test. On the other hand, Chen et al. [28] measured the heat of hydration in cement pastes with limestone-calcined and clay slag. Due to the nature of the samples, the peak values vary, however, the maximum peak heat was obtained between 9 and 15 hours, and the measurement time was approximately 48 hours. The maximum heat value was 1.1 mW/g.

It is observed that the values and times in the graphs vary since all the mixtures do not have the same volumes, the same mixture designs, or the same measurement time. Nevertheless, it can be said that the results obtained by the calorimeter meet the expectations, considering that the behavior of the heat curves obtained corresponds to what has been reported in the literature.

4. Conclusions

Concurrent engineering was used to obtain the optimum design of an adiabatic calorimeter for cementitious mixtures. NSGA-II was used as the optimization algorithm. With the development of this work, it was found that:

(1) One benefit of using NSGA-II to design and construct the adiabatic calorimeter for cement mixtures was the algorithm's ability to work with mixed variables, allowing for the optimization of both the material to be heated and the device's size. The evolutionary algorithms DEMO and MODE, which were tested prior to selecting the optimization algorithm to be employed, were unable to achieve this.

(2) Another benefit was that, unlike the evolutionary algorithms DEMO and MODE, the second objective function permitted the use of design variables with decimal numbers, enabling the convex Pareto front typical of a minimization issue.

(3) It was possible to produce a Pareto front with a convex form, good distribution, and dispersion; this prevented the algorithm from becoming stuck in regionally optimal spots. The diversity of the sample was well preserved across the many simulations thanks to the excellent performance of the agglomeration distance operator for NSGA-II during selection.

(4) The measurement error was lower compared to studies where concurrent engineering was not applied, thus demonstrating the advantage of using optimization algorithms for the design.

(5) The Wilcoxon test was applied, and a value of $p < 0.05$ and a value of $h=1$ were found, indicating the statistical validity of the tests performed.

(6) Among the limitations found when implementing NSGA-II, one of them was its long simulation time, since it took 2 to 3 hours to obtain the Pareto front, increasing the computational cost of using this algorithm.

(7) Also, due to the nature of the process to be optimized, it was not possible to use NSGA-II without modification since it was necessary to create a specific function that included the chosen objective functions.

(8) The novelty of this work is that the calorimeter was developed using concurrent design (optimization algorithms) unlike existing calorimeters. This work is expected to pioneer the development of optimized calorimeters for cement mixtures.

Acknowledgments

Conflicts of Interest

The authors declare no conflict of interest.

References

[1] R. A. Sanderson, G. M. Cann, and J. L. Provis, "Comparison of Calorimetric Methods for the Assessment of Slag Cement Hydration," Advances in Applied Ceramics, vol. 116, no. 4, pp. 186-192, 2017.

[2] W. Wongkeo, P. Thongsanitgarn, C. S. Poon, and A. Chaipanich, "Heat of Hydration of Cement Pastes Containing High-Volume Fly Ash and Silica Fume," Journal of Thermal Analysis and Calorimetry, vol. 138, no. 3, pp. 2065-2075, November 2019.

[3] T. S. Gan, M. Steffan, M. Grunow, and R. Akkerman, "Concurrent Design of Product and Supply Chain Architectures for Modularity and Flexibility: Process, Methods, and Application," International Journal of Production Research, vol. 60, no. 7, pp. 2292-2311, 2021.

[4] M. H. Esfe, M. Hajian, D. Toghraie, M. Khaje khabaz, A. Rahmanian, M. Pirmoradian, et al., "Prediction the Dynamic Viscosity of MWCNT-Al2O3 (30:70)/ Oil 5W50 Hybrid Nano-Lubricant Using Principal Component Analysis (PCA) with Artificial Neural Network (ANN)," Egyptian Informatics Journal, vol. 23, no. 3, pp. 427-436, September 2022.

[5] J. S. Xia, M. K. Khabaz, I. Patra, I. Khalid, J. R. N. Alvarez, A. Rahmanian, et al., "Using Feed-Forward Perceptron Artificial Neural Network (ANN) Model to Determine the Rolling Force, Power and Slip of the Tandem Cold Rolling," ISA Transactions, vol. 132, pp. 353-363, January 2023.

[6] A. Deshpande, "Concurrent Engineering, Knowledge Management, and Product Innovation," Journal of Operations and Strategic Planning, vol. 1, no. 2, pp. 204-231, December 2018.

[7] P. Kügler, F. Dworschak, B. Schleich, and S. Wartzack, "The Evolution of Knowledge-Based Engineering from a Design Research Perspective: Literature Review 2012–2021," Advanced Engineering Informatics, vol. 55, article no. 101892, January 2023.

[8] T. Wang and J. Feng, "Optimal Review Strategy for Concurrent Execution of Design–Construction Tasks in DB Mode," Journal of Construction Engineering and Management, vol. 149, no. 1, article no. 04022139, January 2023.

[9] G. Prasath and M. Santhanam, "Experimental Investigations on Heat Evolution during Hydration of Cementitious Materials in Concrete Using Adiabatic Calorimeter," Indian Concrete Journal, vol. 87, no. 5, pp. 19-28, 2013.

[10] K. A. Riding, J. Vosahlik, K. Bartojay, C. Lucero, A. Sedaghat, A. Zayed, et al., "Methodology Comparison for Concrete Adiabatic Temperature Rise," ACI Materials Journal, vol. 116, no. 2, pp. 45-53, 2019.

[11] B. Klemczak and M. Batog, "Heat of Hydration of Low-Clinker Cements," Journal of Thermal Analysis and Calorimetry, vol. 123, no. 2, pp. 1351-1360, February 2016.

[12] D. Zou, D. Gong, and H. Ouyang, "A Non-Dominated Sorting Genetic Approach Using Elite Crossover for the Combined Cooling, Heating, and Power System with Three Energy Storages," Applied Energy, vol. 329, article no. 120227, January 2023.

[13] G. De Schutter and L. Taerwe, "General Hydration Model for Portland Cement and Blast Furnace Slag Cement," Cement and Concrete Research, vol. 25, no. 3, pp. 593-604, April 1995.

[14] Y. K. Ramu, I. Akhtar, and M. Santhanam, "Use of Adiabatic Calorimetry for Performance Assessment of Concretes," Advances in Cement Research, vol. 28, no. 8, pp. 485-493, September 2016.

[15] E. R. Graeff, "Elevação De Temperatura De Concretos Com Baixo Consumo De Cimento E Adição De Cinza Volante," MS. dissertation, Department Civil Engineering, Universidade Federal de Santa Catarina, Florianópolis, SC, 2017. (In Português)

[16] J. Wang, J. Zhang, and J. Zhang, "Cement Hydration Rate of Ordinarily and Internally Cured Concretes," Journal of Advanced Concrete Technology, vol. 16, no. 7, pp. 306-316, 2018.

[17] S. Verma, M. Pant, and V. Snasel, "A Comprehensive Review on NSGA-II for Multi-Objective Combinatorial Optimization Problems," IEEE Access, vol. 9, pp. 57757-57791, 2021.

[18] H. A. Al-Jamimi, G. M. BinMakhashen, K. Deb, and T. A. Saleh, "Multiobjective Optimization and Analysis of Petroleum Refinery Catalytic Processes: A Review," Fuel, vol. 288, article no. 119678, March 2021.

[19] M. Ayaz, A. Panwar, and M. Pant, "A Brief Review on Multi-Objective Differential Evolution," Soft Computing: Theories and Applications: Proceedings of SoCTA 2018, pp. 1027-1040, 2020.

[20] M. Kalami, "NSGA-II in MATLAB," https://www.yarpiz.com, January 24, 2023.

[21] Y. Wang, Z. Liu, C. Cai, L. Xue, Y. Ma, H. Shen, et al., "Research on the Optimization Method of Integrated Energy System Operation with Multi-Subject Game," Energy, vol. 245, article no. 123305, April 2022.

[22] Y. Zhou, S. Cao, R. Kosonen, and M. Hamdy, "Multi-Objective Optimisation of an Interactive Buildings-Vehicles Energy Sharing Network with High Energy Flexibility Using the Pareto Archive NSGA-II Algorithm", Energy Conversion and Management, vol. 218, article no. 113017, August 2020.

[23] A. Vukadinović, J. Radosavljević, A. Đorđević, M. Protić, and N. Petrović, "Multi-Objective Optimization of Energy Performance for a Detached Residential Building with a Sunspace Using the NSGA-II Genetic Algorithm," Solar Energy, vol. 224, pp. 1426-1444, August 2021.

[24] Z. Babajamali, M. Khaje khabaz, F. Aghadavoudi, F. Farhatnia, S. A. Eftekhari, and D. Toghraie, "Pareto Multi-Objective Optimization of Tandem Cold Rolling Settings for Reductions and Inter Stand Tensions Using NSGA-II," ISA Transactions, vol. 130, pp. 399-408, November 2022.

[25] Y. Lin, "Thermal Stress Analysis for Early Age Mass Concrete Members," Ph.D. dissertation, Department of Civil and Environmental Engineering, West Virginia University, Morgantown, WV, 2015.

[26] S. E. Chidiac and M. Shafikhani, "Cement Degree of Hydration in Mortar and Concrete," Journal of Thermal Analysis and Calorimetry, vol. 138, no. 3, pp. 2305-2313, November 2019.

[27] Y. Lin and H. L. Chen, "Thermal Analysis and Adiabatic Calorimetry for Early-Age Concrete Members," Journal of Thermal Analysis and Calorimetry, vol. 122, no. 2, pp. 937-945, November 2015.

[28] Y. Chen, Y. Zhang, B. Šavija, and O. Çopuroğlu, "Fresh Properties of Limestone-Calcined Clay-Slag Cement Pastes," Cement and Concrete Composites, vol. 138, article no. 104962, April 2023.